Extended Essay

Mathematics

The mathematics behind flat-folding origami and the Miura fold.

Research question:

What are the mathematical properties of the Miura fold that allow flat-folding, and how can the Miura fold be applied?

Candidate number: 000858 0053

Session: May 2020

Extended Essay: Mathematics

Word Count: 3997

Table of contents

Introduction

I have had a fascination with origami ever since I learned how to fold a paper-frog in elementary school. This fold stood out to me for two reasons: when you pressed the back-end of the frog it did a little jump, and it could also be pressed between the pages of my books and brought home without any damage to the shape, unlike other types of origami. More recently I looked into origami with renewed interest, which is how I found the Miura map-fold.

The Miura fold is a fascinating piece of origami, as it can both be folded flat, like the frog, and be opened or closed in a singular motion, giving it a dynamic elegance. This way of folding piqued my interest and led me into the world of flat-folding origami and origami algebra. Wanting a more practical approach as well, I had the idea of looking into how the Miura fold could be incorporated into a product design in order to utilize its unique properties.

This investigation will introduce the concept of the Miura fold, explore the two main theorems within origami algebra related to flat-folding, and apply the characteristics of the Miura fold to a possible design of a foldable sleeping-mat.

Research question

What are the mathematical properties of Miura folds allowing flat-folding, and how can the Miura fold be applied?

Mathematical properties of the Miura fold

Flat folding origami are pieces of origami where the final folded paper can be pressed flat without creating new creases or ruining old ones. In these types of origami folds, there are only two types of creases: the mountain crease and the valley crease (Hull, 1994). By representing the valley creases with dotted lines and the mountain creases with whole lines, a map of the creases of the fold can be created, as shown in Figure 1 and 2.

Figure 1: A flat-folding origami frog

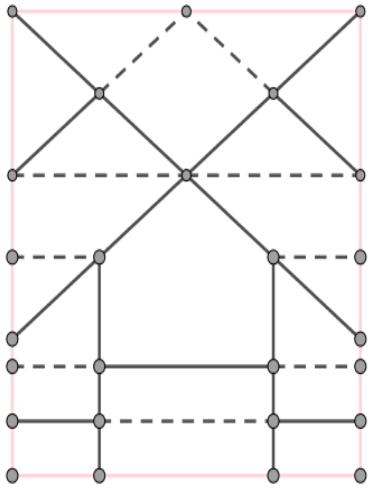

Figure 2: Crease map of a flat-folding origami frog

One type of flat-folding origami is the Miura fold, also called the Miura map-fold and the Miura-ori. The fold was invented in 1985 by Koryo Miura, a Japanese astrophysicist (Garcia, 2017). A Miura fold, as it will be referred to in this essay, is a type of origami fold used to fold flat surfaces into flat folds of smaller surface-area. As with most origami, paper is most commonly used for this. The crease pattern of a Miura fold will look like the one in Figure 3.

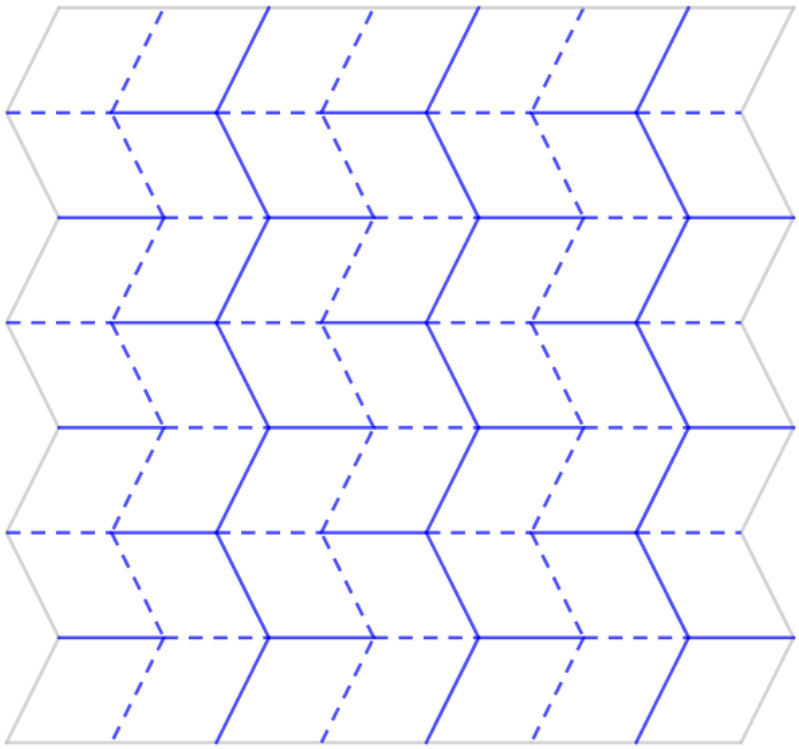

Figure 3: Crease map of a Miura fold

The crease map consists of rows of slanted parallelograms. Where four parallelograms meet, there is a vertex consisting of exactly four joined creases. These vertices either have three mountain creases and one valley crease or three valley creases and one mountain crease. Adjacent rows of parallelograms are slanted in opposite directions, causing the adjacent rows of vertices to look like they are "pointed" in opposite directions (Figure 4).

Figure 4: Vertex pointing to the left (left) and vertex pointing to the right (right)

When folded, the parallelograms combine to form parallelogram- or trapezoid-shapes, sometimes with small triangular gaps, as shown in Figure 5 and 6.

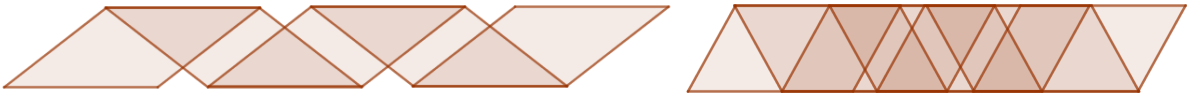

Figure 5: Parallelogram-shape with gaps (left) and without gaps (right)

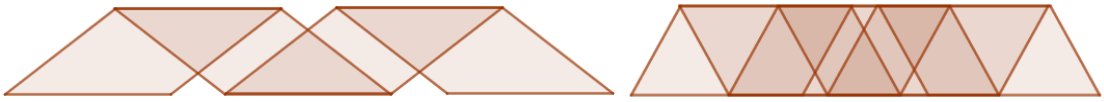

Figure 6: Trapezoid-shape with gaps (left) and without gaps (right)

What is perhaps most notable about the Miura fold is its so-called shape memory. When unfolded, it can be "re-folded and returned to its compact shape" much more easily than other origami folds, flat-folding or not (Garcia, 2017). In the case of the Miura fold, it can be unfolded and re-folded with one diagonal motion between two opposing corners (Figure 7).

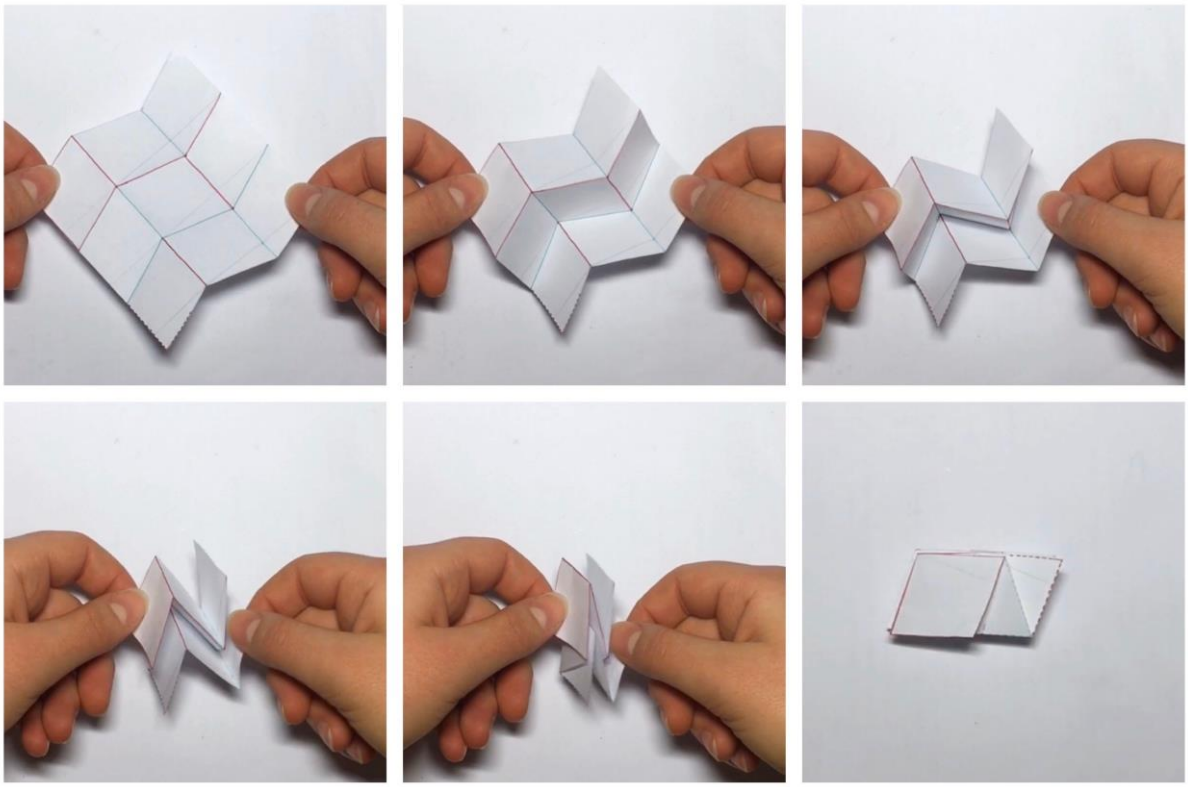

Figure 7: Re-folding a Miura fold in one diagonal motion

This characteristic is part of what makes the Miura fold so interesting, as it has possible, and existing, applications that reach beyond just paper-folding. Before delving into that, I will look at the mathematical properties of flat-folding origami vertices and how these apply to the Miura fold.

Why do Miura folds fold flat?

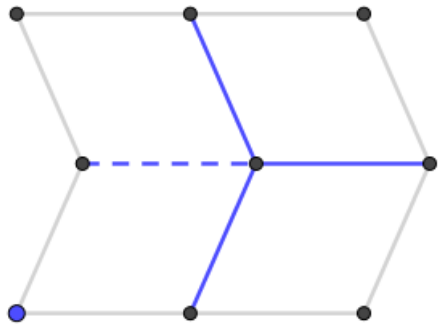

Figure 8: Crease map of a Miura fold vertex

There are certain properties of the creases and angles at the vertices of flat-folding origami pieces that allow them to fold flat. These properties are described by two theorems, namely Maekawa's theorem and Kawasaki's theorem.

Kawasaki's theorem

Kawasaki's theorem states that a vertex can be folded flat if and only if the sum of the alternating angles around it is 180° (Demaine, 2010).

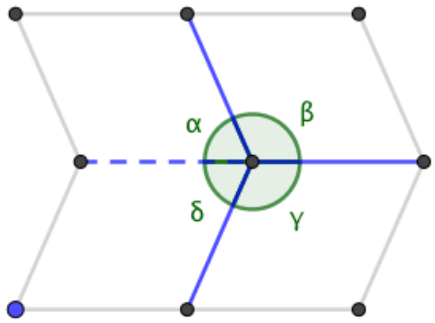

Figure 9: Angles around a Miura fold vertex

For the vertex in Figure 9 to be locally foldable, the following must be true:

$$\alpha + \gamma = 180°$$

$$\beta + \delta = 180°$$

$$\alpha + \gamma - \beta - \delta = 0°$$

In a single vertex of a Miura fold the angles α and β are supplementary and the angles γ and δ are supplementary.

As all the parallelograms in a Miura fold are congruent, the angles α and δ are congruent and the angles β and γ are congruent.

$$\alpha + \beta = \gamma + \delta = 180°$$

$$\alpha = \delta \wedge \beta = \gamma$$

$$\alpha + \gamma = \beta + \delta = 180°$$

$$\alpha + \gamma - \beta - \delta = 0°$$

Therefore, Kawasaki's theorem holds true in all vertices of a Miura fold. Kawasaki's theorem is a necessary condition for a Miura vertex to fold flat, but it is not sufficient to guarantee that it does. Although Kawasaki's theorem reveals if the angles of a vertex facilitate local flat-foldability, it does not mention the folding pattern needed to achieve this flat fold. There is another theorem that narrows down the number of different mountain and valley crease combinations needed for the vertex to be flat foldable, namely Maekawa's theorem.

Maekawa's theorem

Maekawa's theorem states that, when a vertex folds flat, the number of mountain creases and valley creases joined in the vertex always differ by two (Natural Origami, 2016).

$$|M - V| = 2$$

As the Miura fold only has four creases joined at each vertex, it can have a combination of either three mountain creases/one valley crease or three valley creases/one mountain crease. In theory, this would allow for eight different combinations of mountain and valley creases.

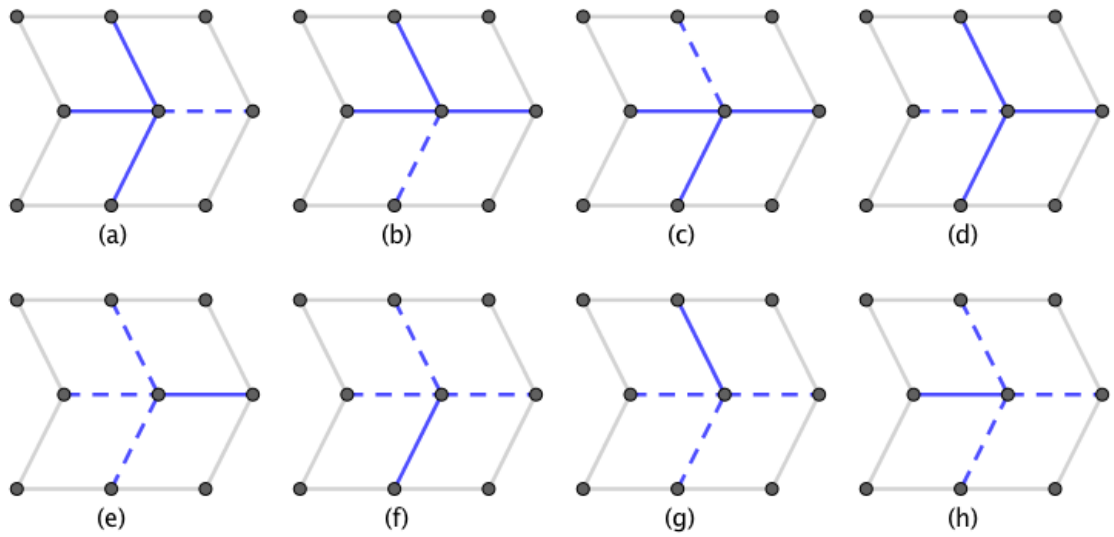

Figure 10: Crease maps of possible mountain/valley combinations in Miura fold vertices

Bird's foot forcing

Only six of these mountain and valley combinations are actually flat foldable. The vertices shown in Figure 10.a and 10.e cannot be folded flat.

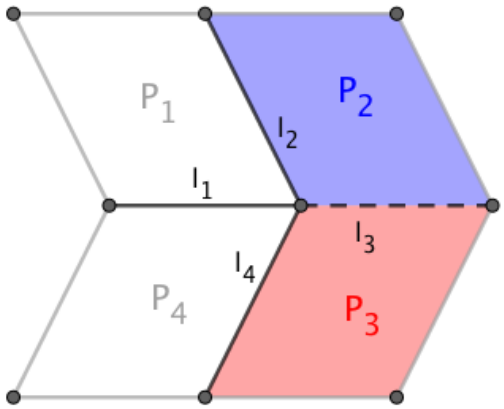

Figure 11: Crease map of a non-foldable Miura fold vertex

Figure 11 shows a scaled-up version of Figure 10.a. In an attempt to fold this vertex according to the crease map, the surface P_2 would have to be folded under P_1 along l_2 to create a mountain fold, while P_3 would have to be folded under P_4 along l_4 to create another mountain fold.

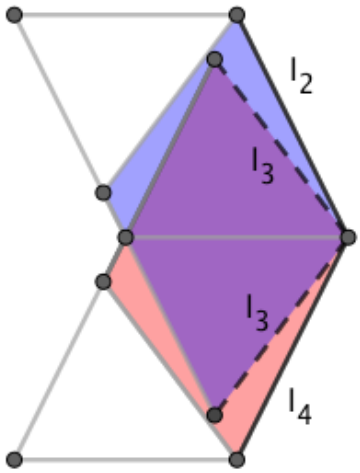

Figure 12: Attempt at folding Figure 11

After folding P_2 and P_3 they would overlap in the purple area shown in Figure 12, but this overlap can only happen by cutting the fold along l_3. There are two possible ways for the vertex to fold flat and l_3 to remain undivided:

1. l_3 could be folded into a mountain crease while l_1 becomes a valley crease, in which case the fold would become the same as in Figure 10.d.
2. l_3 could be folded into a mountain crease while adding two new valley creases (l_5 and l_6). These creases would extend from the vertex, dividing P_2 and P_3 into two parts each (Figure 13). In this case, the vertex consists of more than four creases and does no longer qualify as a Miura fold.

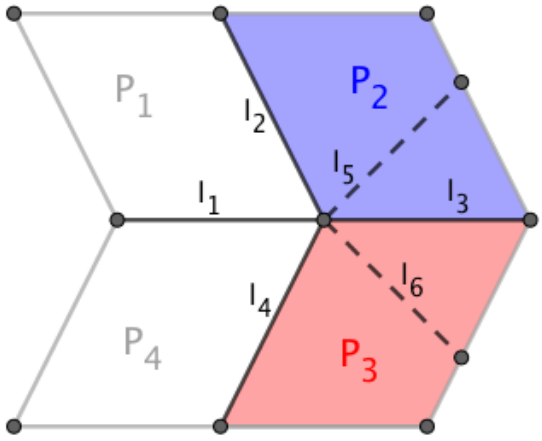

Figure 13: Flat folding of Figure 11

The phenomenon of not being able to fold flat using the crease pattern in Figure 10.a and 10.e is called bird's foot forcing due to the vertex's visual similarity to a bird's foot (Hull and Ginepro, 2014).

Not all vertexes shown in Figure 10 can be folded flat, even though both Maekawa's theorem and Kawasaki's theorem hold true in all of them. This shows that both Maekawa's theorem and Kawasaki's theorem are necessary but insufficient conditions for a vertex to have flat foldability.

By looking at a standard Miura fold with multiple vertices (Figure 14), it becomes apparent that only the mountain/valley pairings shown in Figure 10.d and 10.h are present.

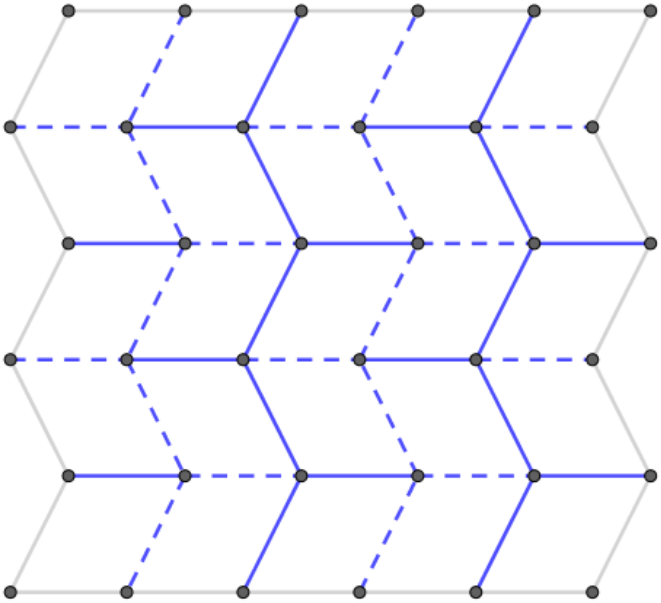

Figure 14: Standard Miura fold with five by five parallelograms

Both Maekawa's theorem and Kawasaki's theorem hold true in the vertices of the Miura fold, and, due to the absence of the bird's foot forcing, they all have local flat-foldability. Local flat-foldability in all the vertices of a fold do not guarantee global flat-foldability (Hull, 1994). However, the alternating pattern of creases and vertices in the Miura fold allow for global flat-foldability.

Application of the Miura fold

The intention of the original Miura fold was to be a design used for solar panels in space, as they could be stored folded during the launch and easily opened when the probe reached its intended orbit (Landau, 2017) (Garcia, 2017). The fold has also been used to fold maps to make them easier to refold when opened, hence the name Miura map-fold (Bain, 1980). Another area where one could potentially make use of the characteristics of the Miura map-fold is sleeping-mats. Sleeping-mats used for hiking are typically made of foam and have to be rolled up after use. They take a lot of space, as the rolled-up mat is left with an empty cylinder in the middle. There are existing sleeping-mat designs which are foldable (Figure 15) and there are sit pads making use of a fold visually similar to a Miura vertex, just with squares or rectangles instead of parallelograms (Figure 16).

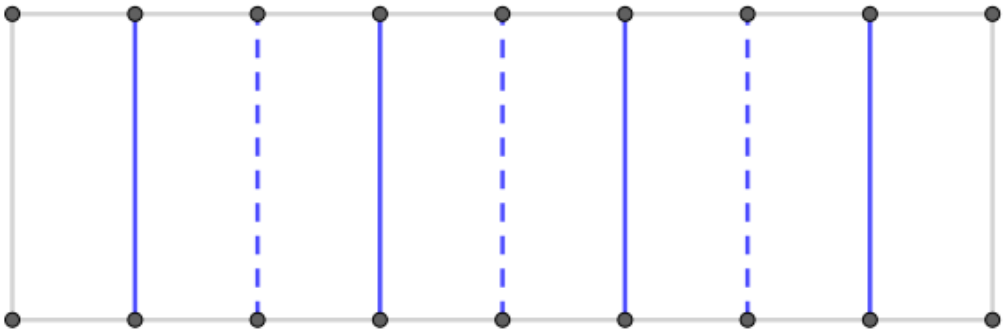

Figure 15: Crease map of a folded sleeping-mat

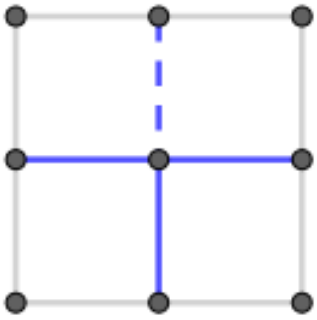

Figure 16: Crease map of a sit pad

By utilising the Miura fold it might be possible to create a foldable sleeping-mat that occupies less space and takes less effort to pack and unpack. The first step in doing so would be to determine the relationship between the area of the folded and unfolded Miura fold. In order to do this, I opted to use GeoGebra to create models of both the folded and unfolded version of a single Miura vertex.

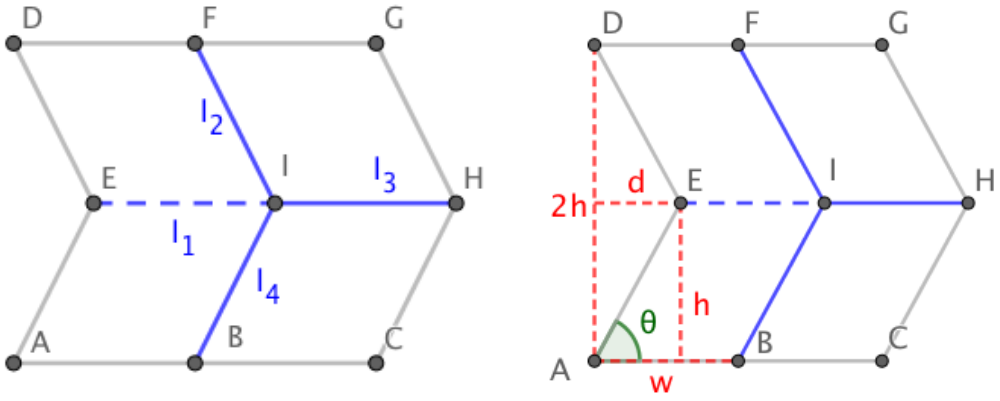

Figure 17: Unfolded Miura vertex

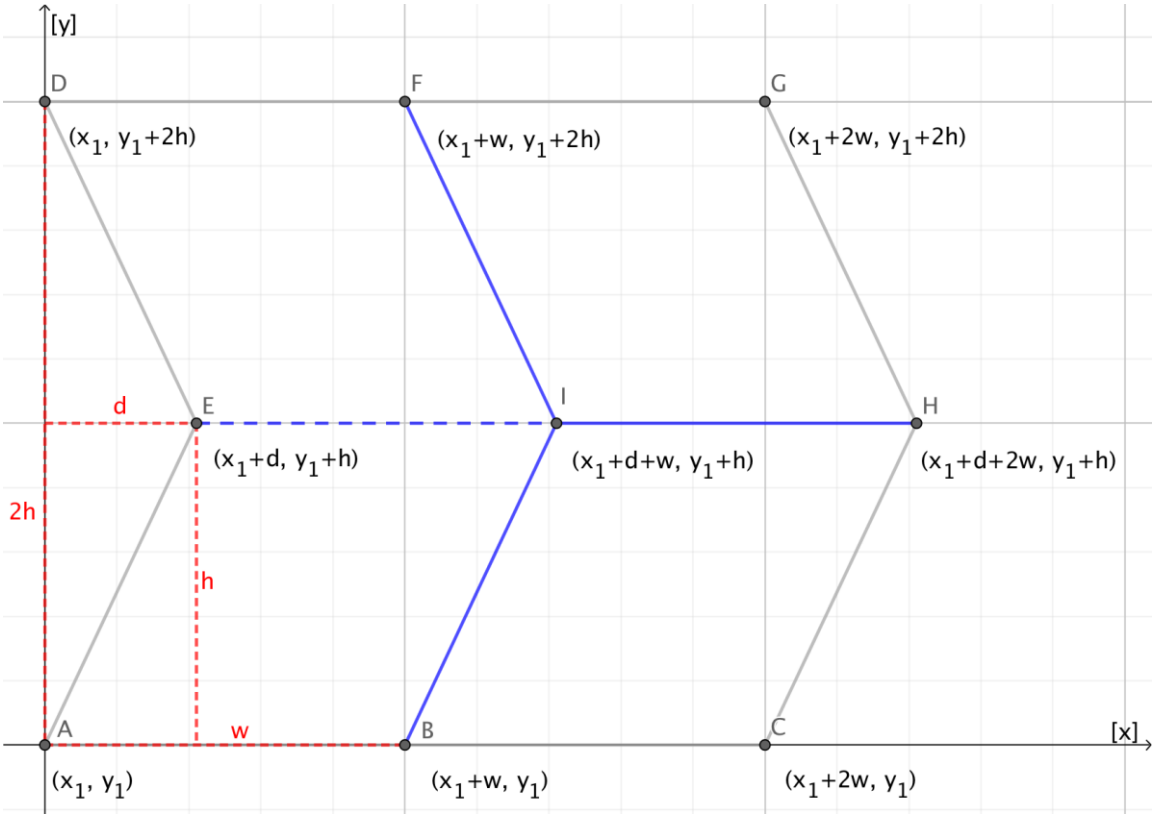

Figure 18: Unfolded Miura vertex with distances and coordinates

The base of the vertex is the parallelogram ABIE (Figure 17). The point A has the coordinates (x_1, y_1). The length of the segment AB is *w*. The vertical distance from point A to point E is *h*. The horizontal distance from point A to point E is *d*. The coordinates of remaining points are shown in Figure 18.

The values *w*, *d*, and *h* are all variables and are represented by sliders in the GeoGebra model.

Table 1: Table of coordinates of the points from Figure 17 and 18

A:	(x_1, y_1)
B:	(x_1+w, y_1)
C:	(x_1+2w, y_1)
D:	(x_1, y_1+2h)
E:	(x_1+d, y_1+h)
F:	(x_1+w, y_1+2h)
G:	(x_1+2w, y_1+2h)
H:	(x_1+d+2w, y_1+h)
I:	(x_1+d+w, y_1+h)

The folded Miura vertex is represented by the model shown in Figure 20. The grey lines show the edges of the paper, while the blue lines represent the folds. The dashed line still represents the valley crease, but, after folding, this crease is inside the fold and not visible from the outside. Each point in Figure 19 corresponds to the point of the same letter in Figure 17.

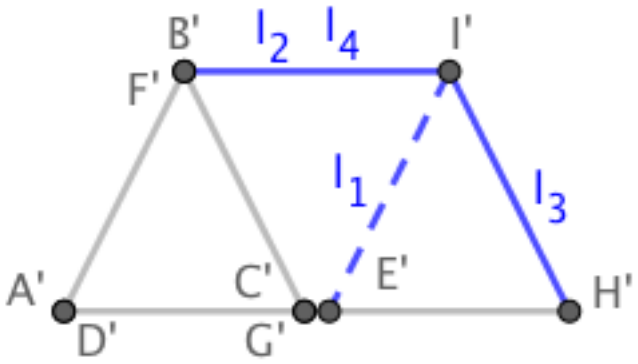

Figure 19: Folded version of the Miura vertex in Figure 17

In Figure 19, the lines l_2 and l_4 from Figure 17 are now directly behind each other. The parallelograms ABIE and EIFD (Figure 17) completely overlap in Figure 19, and so do the parallelograms BCHI and IHGF, meaning there are now three double points: A' and D', C' and G', and B' and F'.

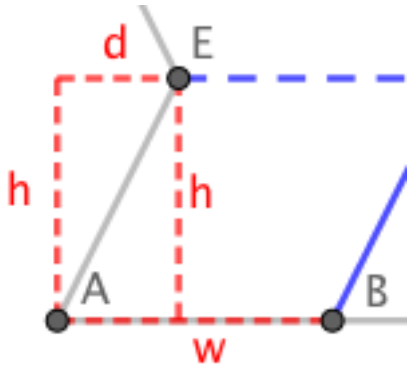

Figure 20: Closeup of Figure 18

The area of a folded Miura vertex

The geometric shape of the fold in Figure 15 is called an isosceles trapezoid. The area of an isosceles trapezoid is given by the formula (Weisstein, 2019):

$$Area = \frac{top + bottom}{2} \times height$$

In order to apply this formula to Figure 19, one has to know the height as well as the length of the top and bottom line of the trapezoid. Therefore, the lengths of the segments A'E' and A'C' have to be determined, as well as the segment A'Q (Figure 21).

Knowing the vertical and horizontal distance from A to E (Figure 17), Pythagoras can be used to determine the length of the segment AE.

$$c^2 = a^2 + b^2$$

$$AE = \sqrt{h^2 + d^2}$$

The length of AE is the same as the length of BI and CH.

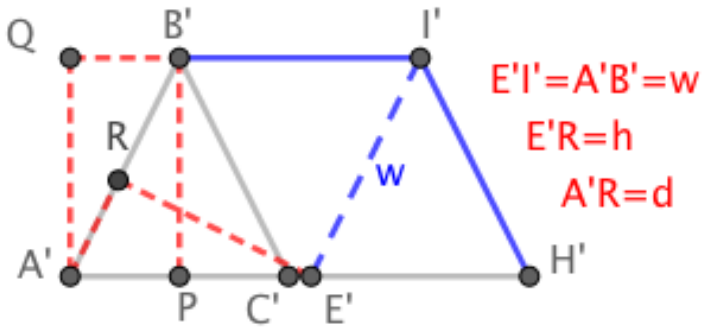

Figure 21: Folded Miura vertex from Figure 17 with distances

The length of the segment A'C' (Figure 21) can be found using the trigonometric functions.

$$\angle B'A'P = \angle RA'E'$$

$$\frac{E'R}{A'R} = \frac{h}{d} = \tan(\angle RA'E')$$

$$\angle B'A'P = \tan^{-1}\left(\frac{h}{d}\right)$$

$$\frac{A'P}{A'B'} = \frac{A'P}{w} = \cos(\angle B'A'P) = \cos\left(\tan^{-1}\left(\frac{h}{d}\right)\right)$$

$$A'P = w \times \cos\left(\tan^{-1}\left(\frac{h}{d}\right)\right)$$

$$A'C' = 2 \times A'P$$

$$A'C' = 2w\cos\left(\tan^{-1}\left(\frac{h}{d}\right)\right)$$

The height of the fold is the segment A'Q (Figure 21), which is the same length as the vertical distance from A' to B'. This height can be found using the trigonometric function.

$$A'Q = B'P$$

$$\angle B'A'P = \tan^{-1}\left(\frac{h}{d}\right)$$

$$\frac{B'P}{A'B'} = \frac{B'P}{w} = \sin(\angle B'A'P) = \sin\left(\tan^{-1}\left(\frac{h}{d}\right)\right)$$

$$B'P = A'Q = w \times \sin\left(\tan^{-1}\left(\frac{h}{d}\right)\right)$$

However, figuring out the length of the bottom of the fold introduces certain complications due to the gaps that appear in some versions of the Miura fold, as shown in Figure 5 and 6. The following section will focus on avoiding this gap.

Uncomplicating the folded figure

In the isosceles trapezoid shown in Figure 19, the segments A'E' and C'H' have an overlap. This is not always the case when a Miura fold is folded. Depending on the values of *h*, *w*, and *d*, segments A'E' and C'H' will sometimes be adjacent (Figure 22) or have some distance between them (Figure 23).

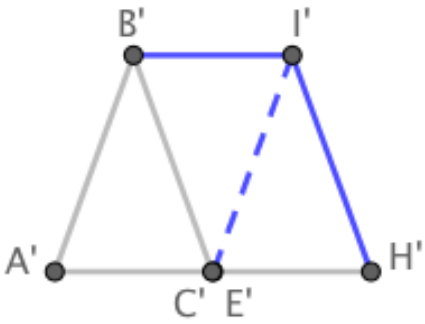

Figure 22: A'E' and C'H' are adjacent

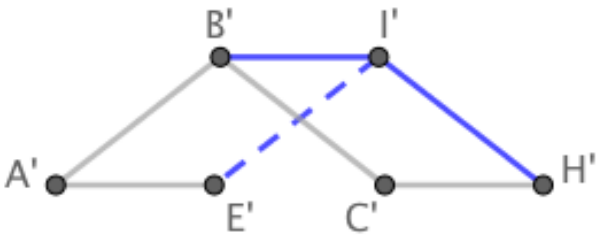

Figure 23: A'E' and C'H' do not overlap and are not adjacent

A gap such as the one in Figure 23 complicates the calculation of the area, as the shape is no longer a trapezoid. In order to avoid this gap, it first has to be determined when point C' and point E' have the same coordinates.

The coordinates of point A' are (x_2, y_2).

As the length of both A'C' and A'E' have already been worked out, the coordinates of point E' and point C' are:

$$E': \left(x_2 + \sqrt{h^2 + d^2}, y_2\right)$$

$$C': \left(x_2 + 2w\cos\left(\tan^{-1}\left(\frac{h}{d}\right)\right), y_2\right)$$

From this, we can determine that when the x-coordinate of point E' is greater than that of point C', there is an overlap.

$$2w\cos\left(\tan^{-1}\left(\frac{h}{d}\right)\right) < \sqrt{h^2 + d^2}$$

When the x-coordinates of point E' and C' are the same, the segments A'E' and C'H' are adjacent.

$$2w\cos\left(\tan^{-1}\left(\frac{h}{d}\right)\right) = \sqrt{h^2 + d^2}$$

When the x-coordinate of point C' is greater than that of point E', there is a gap.

$$2w\cos\left(\tan^{-1}\left(\frac{h}{d}\right)\right) > \sqrt{h^2 + d^2}$$

Hence, there is no gap when the x-coordinate of point E' is greater than or equal to the x-coordinate of point C'.

$$2w\cos\left(\tan^{-1}\left(\frac{h}{d}\right)\right) \leq \sqrt{h^2 + d^2}$$

Through varying the sliders in the GeoGebra model, I observed that with some lengths of w and h there would never be a gap no matter the size of d.

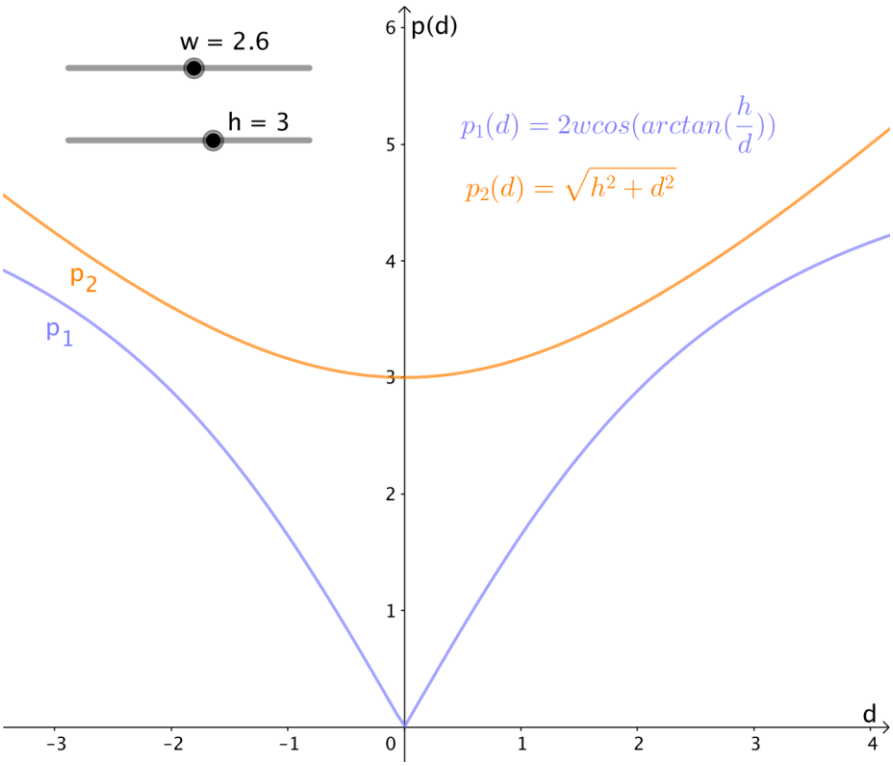

Figure 24: GeoGebra model with w < h

When *w* is less than *h*, p_2 is always greater than p_1, hence there is no gap between A'E' and C'H' (Figure 24).

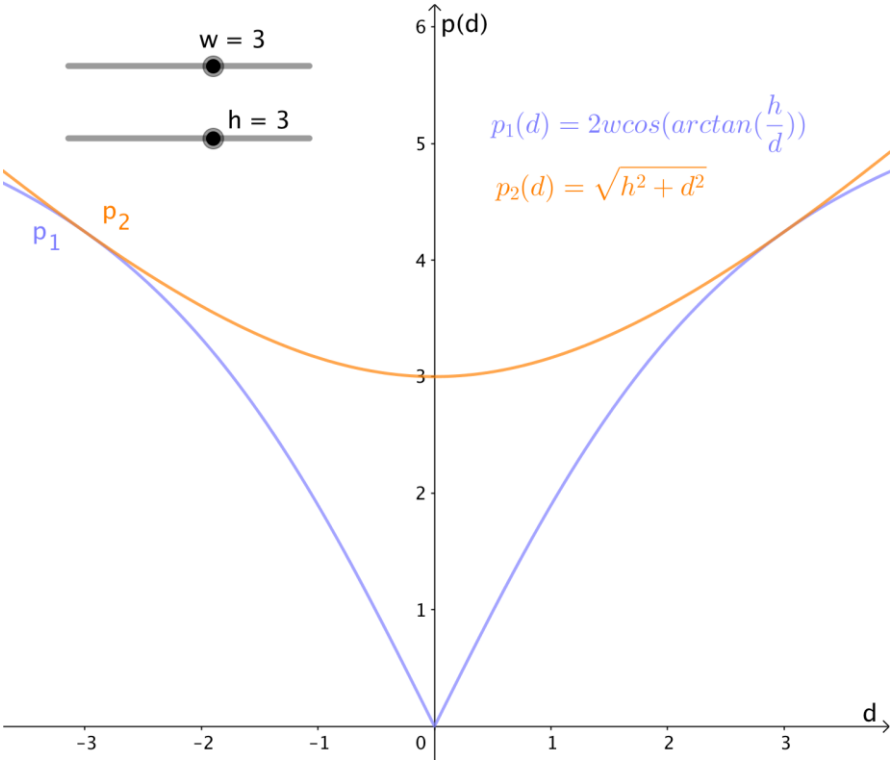

Figure 25: GeoGebra model with w = h

When *w* is equal to *h*, there is no gap between A'E' and C'H'. At two points p_1 and p_2 intersect and are tangent to each other, which is where A'E' and C'H' are adjacent (Figure 25).

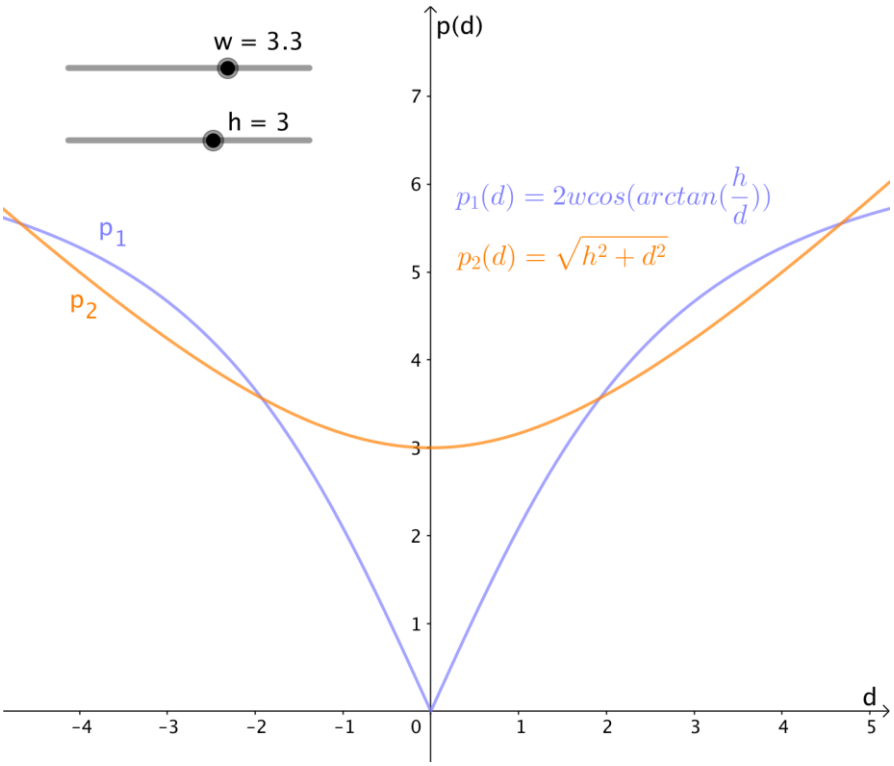

Figure 26: GeoGebra model with w > h

When *w* is greater than *h*, p_1 and p_2 intersect at four points. There is a gap between A'E' and C'H' at the values of *d* where p_1 is greater than p_2 (Figure 26).

Having made these observations, the next step is to prove mathematically that there is never a gap when the value of *w* is less than or equal to the value of *h*.

The equation developed above can be used to figure out the relationship between *h*, *w*, and whether or not there is a gap.

$$2w\cos\left(\tan^{-1}\left(\frac{h}{d}\right)\right) \leq \sqrt{h^2 + d^2}$$

$$4w^2\cos^2\left(\tan^{-1}\left(\frac{h}{d}\right)\right) \leq h^2 + d^2$$

Proof of $\cos^2(\arctan(x)) = 1/(1+x^2)$

The equation can be simplified by using the trigonometric functions:

$$\tan(\tan^{-1}(x)) = x$$

$$\tan^2(\tan^{-1}(x)) = x^2$$

$$1 + \tan^2(\tan^{-1}(x)) = 1 + x^2$$

$$1 + \tan^2(\tan^{-1}(x)) = \sec^2(\tan^{-1}(x))$$

$$\sec^2(\tan^{-1}(x)) = 1 + x^2$$

$$\sec^2(\tan^{-1}(x)) = \frac{1}{\cos^2(\tan^{-1}(x))}$$

$$1 + x^2 = \frac{1}{\cos^2(\tan^{-1}(x))}$$

$$\cos^2(\tan^{-1}(x)) = \frac{1}{1 + x^2}$$

When applied to the equation:

$$4w^2 \cos^2\left(\tan^{-1}\left(\frac{h}{d}\right)\right) = \frac{4w^2}{1 + \frac{h^2}{d^2}}$$

$$\frac{4w^2}{1 + \frac{h^2}{d^2}} \leq h^2 + d^2$$

$$\frac{4w^2 d^2}{d^2 + h^2} \leq h^2 + d^2$$

$$4w^2 d^2 \leq (h^2 + d^2)^2$$

$$4w^2 d^2 \leq h^4 + 2h^2 d^2 + d^4$$

There are too many variables in this equation. There should ideally only be one: the angle θ of the parallelogram (Figure 17). This angle has earlier been expressed in the form of:

$$\theta = \angle \mathrm{B'A'P} = \tan^{-1}\left(\frac{h}{d}\right)$$

Assuming that the height h and width w of the parallelograms will be kept constant, θ will change by changing d. Their exact relationship is:

$$d = \frac{h}{\tan\theta}$$

So, d will be the variable.

$$4w^2d^2 \leq h^4 + 2h^2d^2 + d^4$$

$$0 \leq h^4 + 2h^2d^2 + d^4 - 4w^2d^2$$

$$0 \leq h^4 + 2d^2(h^2 - 2w^2) + d^4$$

There will be no gap between the segments when $h^4 + 2d^2(h^2 - 2w^2) + d^4$ is greater than or equal to zero.

This function can be expressed as a quadratic function by replacing d^2 with n:

$$n^2 + 2(h^2 - 2w^2)n + h^4$$

The quadratic formula can be used to find the roots.

$$n = \frac{-2(h^2 - 2w^2) \pm \sqrt{\left(2(h^2 - 2w^2)\right)^2 - 4 \times 1 \times h^4}}{2 \times 1}$$

The quadratic equation can either have one real root, two real roots, or no real roots. The condition of the number of roots is the value of the discriminant.

When the graph of $n^2 + 2(h^2 - 2w^2) \times n + h^4$ is tangent to the x-axis, there is only one root.

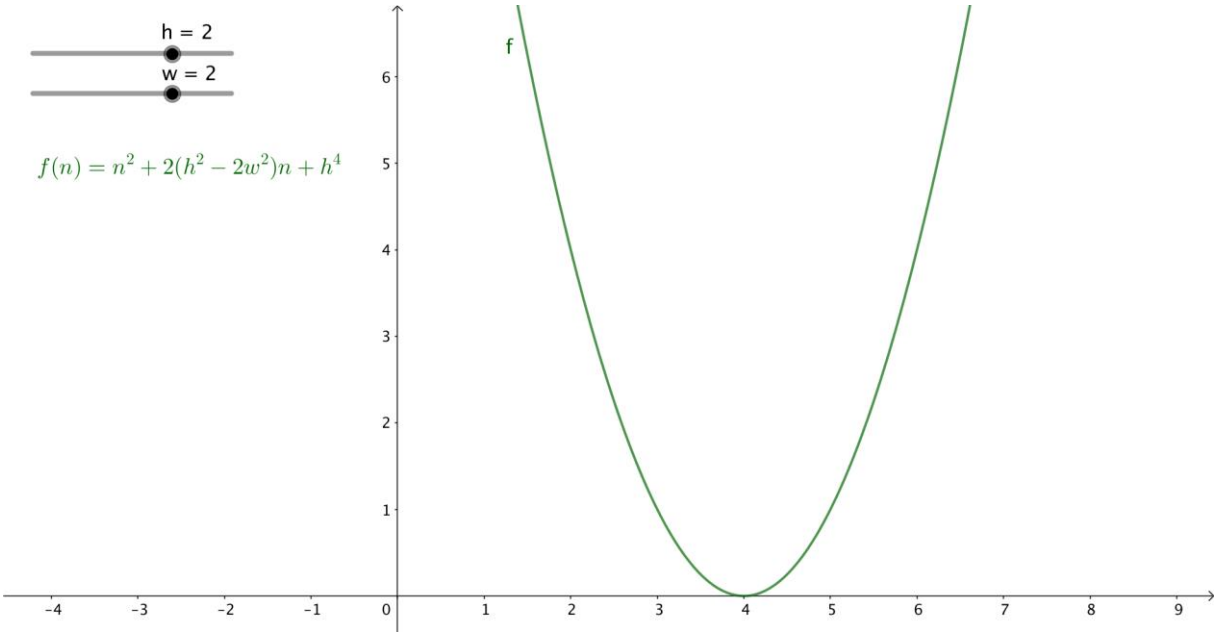

Figure 27: Graph of $n^2+2(h^2-2w^2)n+h^2$ when h = w

To either be tangent to the x-axis or not cross it at all, the discriminant has to be less than or equal to zero.

$$\left(2(h^2 - 2w^2)\right)^2 - 4 \times 1 \times h^4 \leq 0$$

$$4(h^2 - 2w^2)^2 - 4h^4 \leq 0$$

$$4(h^4 - 4h^2w^2 + 4w^4) - 4h^4 \leq 0$$

$$4h^4 - 16h^2w^2 + 16w^4 - 4h^4 \leq 0$$

$$-16(h^2w^2 - w^4) \leq 0$$

$$h^2w^2 - w^4 \geq 0$$

$$w^2(h^2 - w^2) \geq 0$$

The width squared is always greater than zero:

$$w^2 > 0$$

$$h^2 - w^2 \geq 0$$

$$h^2 \geq w^2$$

$$|h| \geq |w|$$

The absolute value of *h* has to be greater than or equal to the absolute value of *w* in order for there to be no gaps in the folded Miura fold.

As both *h* and *w* will be positive in further calculations, there will be no gaps in the final Miura fold when *h* is greater than or equal to *w*. For simplicity's sake, the values of *h* and *w* will be considered equal from now on and referred to as the constant *k*.

Finalizing the function

Now that the condition for there to be no gaps in the fold has been instated, the area of the folded vertex can be calculated. The area of an isosceles trapezoid is found by the formula:

$$Area = \frac{top + bottom}{2} \times height$$

The height is $w \times \sin\left(\tan^{-1}\left(\frac{h}{d}\right)\right)$ and the length of the top is $\sqrt{h^2 + d^2}$, so what remains is an expression for the length of the bottom.

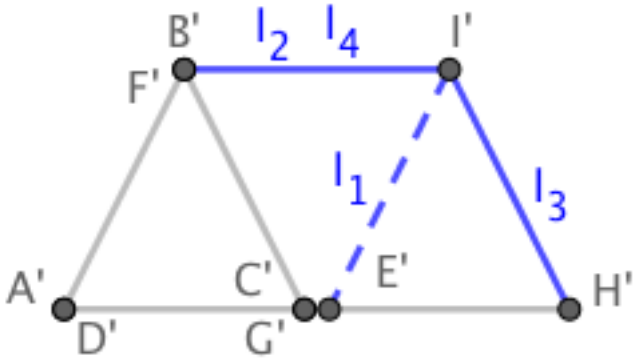

Figure 28: Copy of Figure 19

Unless the segments A'E' and C'H' from Figure 28 are adjacent, which they only are at certain values of *d*, the overlap C'E' must still be considered when working out the area of the trapezoid.

The length of the bottom of the shape is the segment A'H'.

The length of the overlap C'E' between A'E' and C'H' is equal to the x-coordinate of E' minus the x-coordinate of C'.

$$C'E' = \sqrt{k^2 + d^2} - 2k\cos\left(\tan^{-1}\left(\frac{k}{d}\right)\right)$$

The length of the bottom of the trapezoid can be expressed as:

$$A'H' = A'E' + C'H' - C'E'$$

$$A'H' = \sqrt{k^2 + d^2} + \sqrt{k^2 + d^2} - \left(\sqrt{k^2 + d^2} - 2k\cos\left(\tan^{-1}\left(\frac{k}{d}\right)\right)\right)$$

$$A'H = \sqrt{k^2 + d^2} + 2k\cos\left(\tan^{-1}\left(\frac{k}{d}\right)\right)$$

Now, having expressions for the height, the length of the top, and the length of the bottom of the isosceles trapezoid, an expression can be made for its area.

$$Area = \frac{top + bottom}{2} \times height$$

$$A(d) = \frac{\sqrt{k^2 + d^2} + \sqrt{k^2 + d^2} + 2k\cos\left(\tan^{-1}\left(\frac{k}{d}\right)\right)}{2} \times k\sin\left(\tan^{-1}\left(\frac{k}{d}\right)\right)$$

Simplified:

$$A(d) = \left(\sqrt{k^2 + d^2} + k\cos\left(\tan^{-1}\left(\frac{k}{d}\right)\right)\right) \times k\sin\left(\tan^{-1}\left(\frac{k}{d}\right)\right)$$

As shown earlier:

$$\cos(\tan^{-1}(x)) = \frac{1}{\sqrt{x^2 + 1}}$$

The sine of the arctan of x can also be expressed in a similar manner:

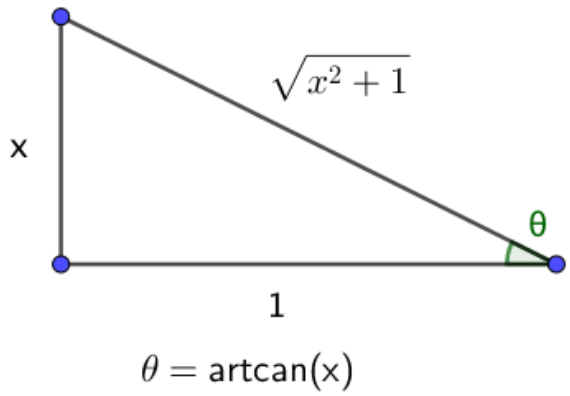

Figure 29: Simplifying sin(arctan(x))

$$\sin(\theta) = \sin(\tan^{-1}(x)) = \frac{x}{\sqrt{x^2+1}}$$

As a result, A(d) can be simplified to:

$$A(d) = \frac{k^2(k^2+kd+d^2)}{k^2+d^2}$$

Plotting this function into GeoGebra gives a graph illustrating how the area of the fold changes as d increases:

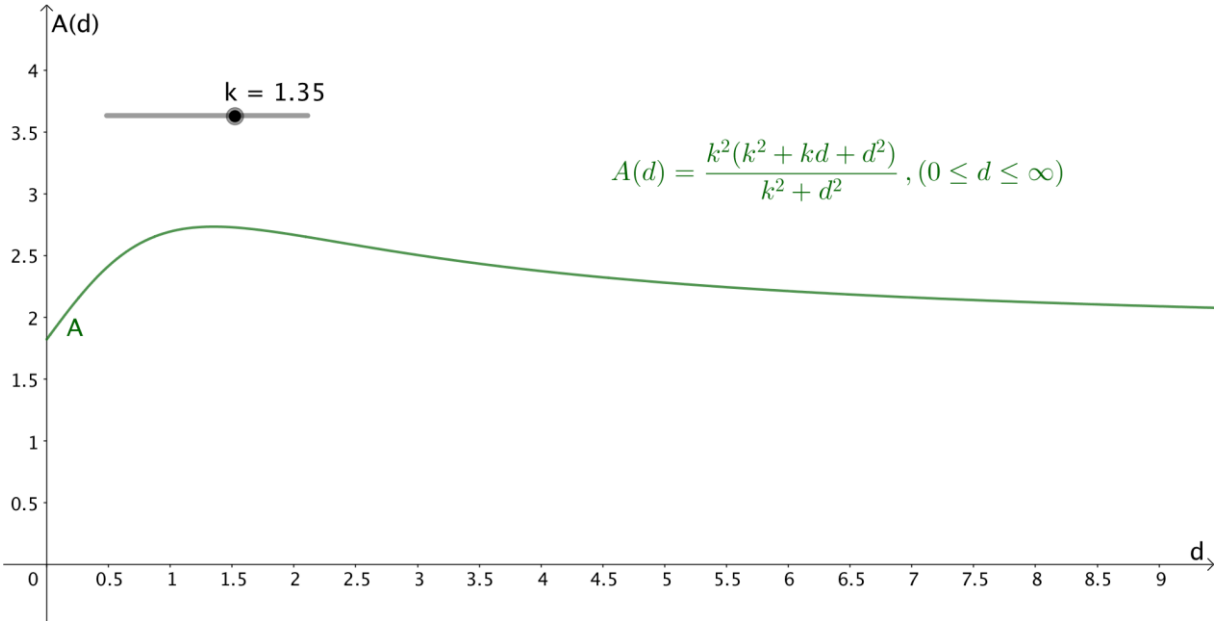

Figure 30: Graph of A(d)

A(d) has a maximum point when $d = k$

A(d) has a horizontal asymptote at $y = k^2$

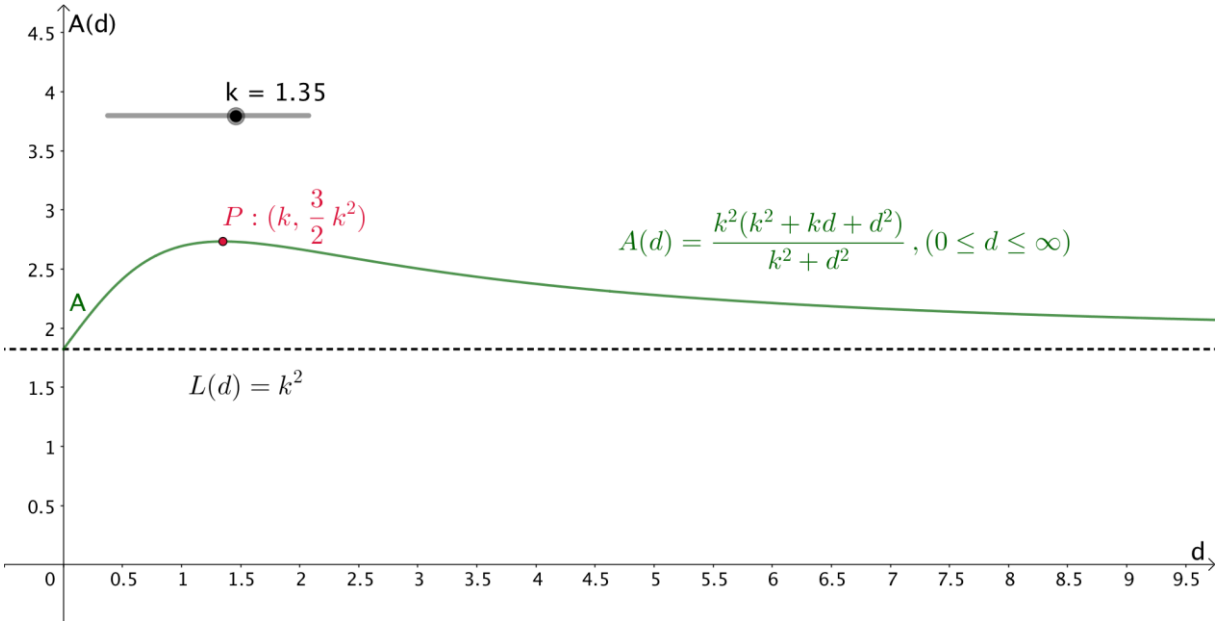

Figure 31: A(d) with maximum and horizontal asymptote

Expanding beyond one vertex

Up until this point only the fold of a single vertex has been considered. As seen in Figure 14 (page 11), a Miura fold can consist of more than just four parallelograms.

The number of horizontal parallelograms, when the unfolded Miura fold is oriented as in Figure 14, determines the length of the top and bottom of the parallelograms. When there is an odd number of horizontal parallelograms the fold has the shape of a parallelogram.

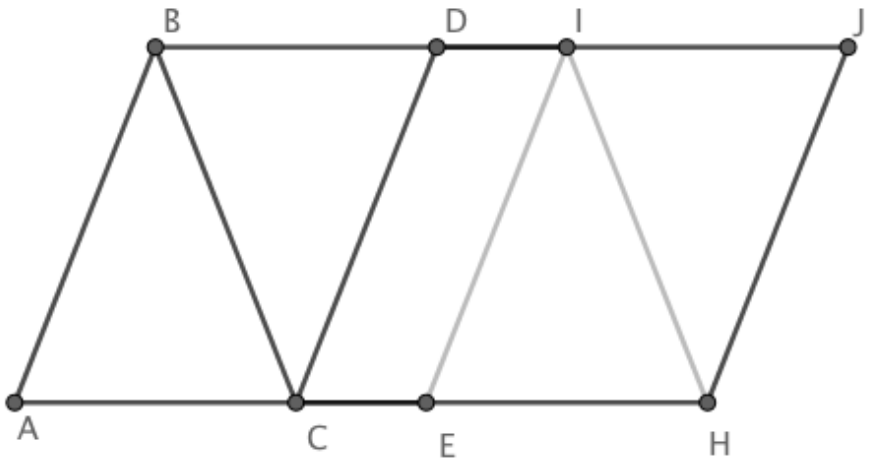

Figure 32: Miura fold with three horizontal parallelograms (grey lines are enclosed in the fold)

For an odd-numbered Miura fold, the length of both the top and the bottom of the fold is the same and can be written as:

$$(n-1)\times\left(\sqrt{k^2+d^2}\right)-(n-2)\times\left(\sqrt{k^2+d^2}-2k\cos\left(\tan^{-1}\left(\frac{k}{d}\right)\right)\right)$$

where *n* is the number of parallelograms horizontally.

The area of a parallelogram is the height times the width, hence the area of a Miura fold with an odd number of parallelograms is:

$$Area = width \times height$$

$$A(d)=\left((n-1)\times\left(\sqrt{k^2+d^2}\right)-(n-2)\times\left(\sqrt{k^2+d^2}-2k\cos\left(\tan^{-1}\left(\frac{k}{d}\right)\right)\right)\right)\times k\sin\left(\tan^{-1}\left(\frac{k}{d}\right)\right)$$

Simplified:

$$A(d)=\frac{k^2(d^2+2nkd-4kd+k^2)}{k^2+d^2}$$

A(d) has a maximum point when $d = k$

A(d) has a horizontal asymptote at $y = k^2$

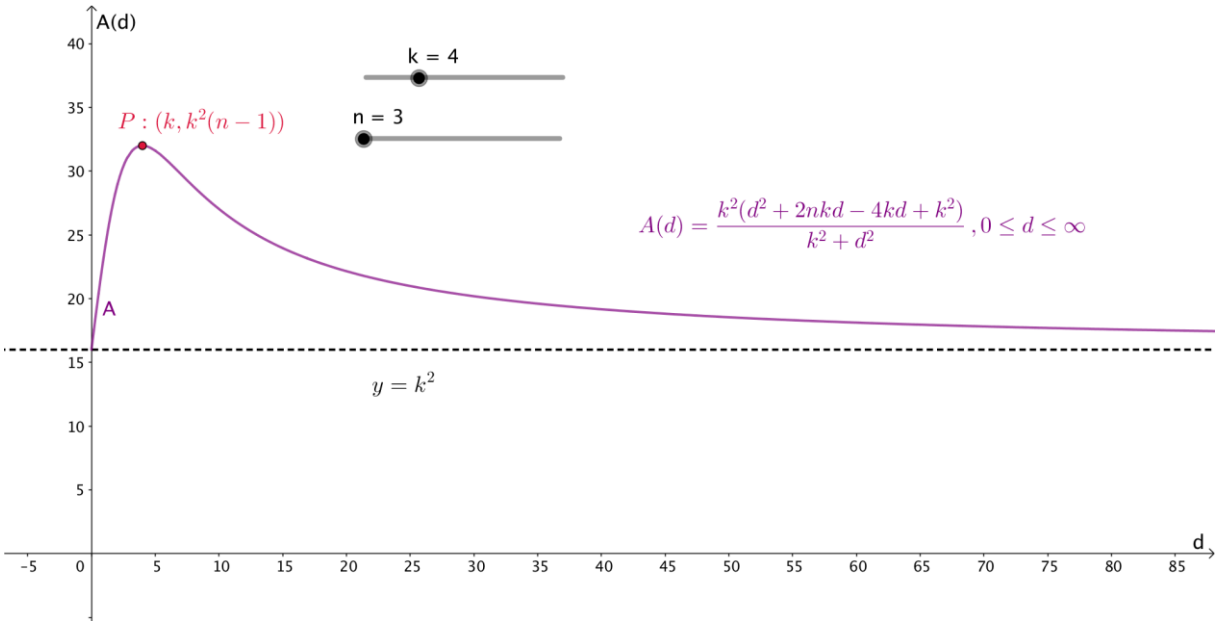

Figure 33: Area of an odd-numbered Miura fold

When there is an even number of horizontal parallelograms, the fold has the shape of an isosceles trapezoid.

For an even-numbered Miura fold, the length of the bottom of the trapezoid is:

$$n \times \left(\sqrt{k^2 + d^2}\right) - (n-1) \times \left(\sqrt{k^2 + d^2} - 2k \cos\left(\tan^{-1}\left(\frac{k}{d}\right)\right)\right)$$

And the length of the top of the trapezoid is:

$$(n-1) \times \left(\sqrt{k^2 + d^2}\right) - (n-2) \times \left(\sqrt{k^2 + d^2} - 2k \cos\left(\tan^{-1}\left(\frac{k}{d}\right)\right)\right)$$

Substituting this into the formula for the area of an isosceles trapezoid gives:

$$A(d) = \frac{n \times \left(\sqrt{k^2 + d^2}\right) - (n-1) \times \left(\sqrt{k^2 + d^2} - 2k \cos\left(\tan^{-1}\left(\frac{k}{d}\right)\right)\right) + (n-1) \times \left(\sqrt{k^2 + d^2}\right) - (n-2) \times \left(\sqrt{k^2 + d^2} - 2k \cos\left(\tan^{-1}\left(\frac{k}{d}\right)\right)\right)}{2} \times k \sin\left(\tan^{-1}\left(\frac{k}{d}\right)\right)$$

Simplified:

$$A(d) = \frac{k^2(d^2 + 2knd - 3kd + k^2)}{k^2 + d^2}$$

A(d) has a maximum point when $d = k$

A(d) has a horizontal asymptote at $y = k^2$

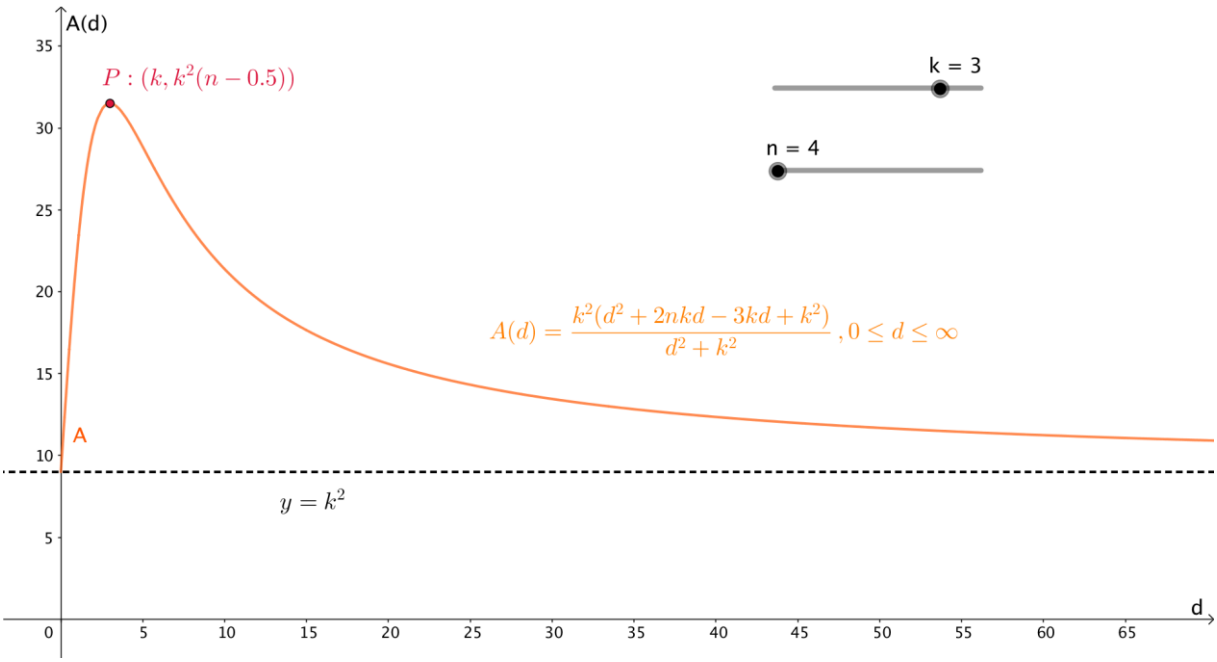

Figure 34: Area of an even-numbered Miura fold

Applying the functions

Now that two functions for the possible areas of the Miura fold have been developed, the number of parallelograms and their size must be determined.

The sleeping-mat I already own has the measurements 186 cm x 60 cm x 1.4 cm. A length of 180 cm would be enough, so the total height of the parallelograms in the unfolded Miura sleeping-mat should add up to 180 cm, while the total width should add up to 60cm.

$$180 = n_1 \times k$$

$$60 = n_2 \times k$$

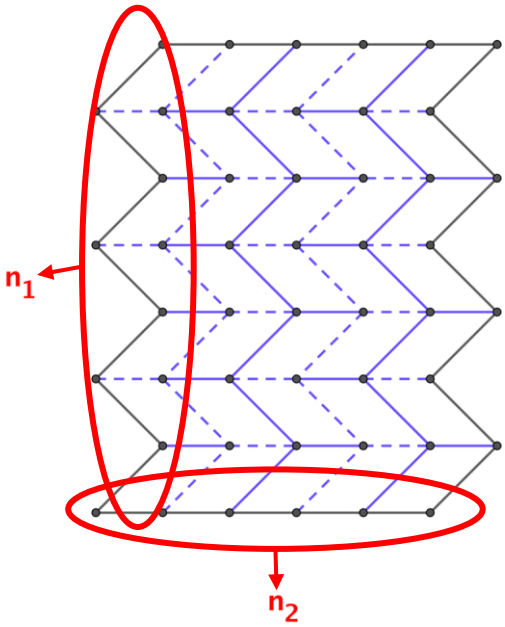

Figure 35: n_1 and n_2

The number of parallelograms vertically is n_1.

The number of parallelograms horizontally is n_2.

k must therefore be a common factor of 180 and 60.

$$180 = 2 \times 2 \times 3 \times 3 \times 5$$

$$60 = 2 \times 2 \times 3 \times 5$$

The possible values of *k* are 2, 3, 4, 5, 6, 10, 12, 15, 20, and 30 cm.

At the lengths 2, 3, 5, 6, 10, 15, and 30 cm, the folded mat will be an isosceles trapezoid. At the lengths 4, 12, and 20 cm, the folded mat will be a parallelogram.

The aim is to find the minimum area, and this would necessitate there existing a minimum area. In Figure 33 and 34 there is a maximum, and there is a horizontal asymptote which the function approaches as d increases, and the only minimum within in the stated range (0 to $+\infty$) is when $d = 0$. When d equals zero, the Miura fold is made up of squares instead of slanted parallelograms (Figure 36).

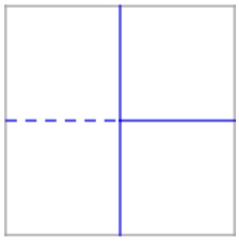

Figure 36: Unfolded Miura fold with d=0

When the Miura fold consists of squares, it loses its characteristic of being foldable with one diagonal motion, which is one of the essential properties of the Miura fold required for the sleeping-mat design. As a result, neither the equation for the odd- nor even-numbered Miura folds has a minimum point which satisfies the criterion of the fold being a Miura fold. Hence, a minimum area cannot be found.

Optimizing the volume

As a minimum area cannot be found, other factors should be considered, such as the volume of the folded mat. The mat itself will have a thickness of about 1.5 cm, so how much it is being folded will affect its total volume. The thickness of the folded mat is determined by the number of parallelograms, both horizontally and vertically, and how tilted they are.

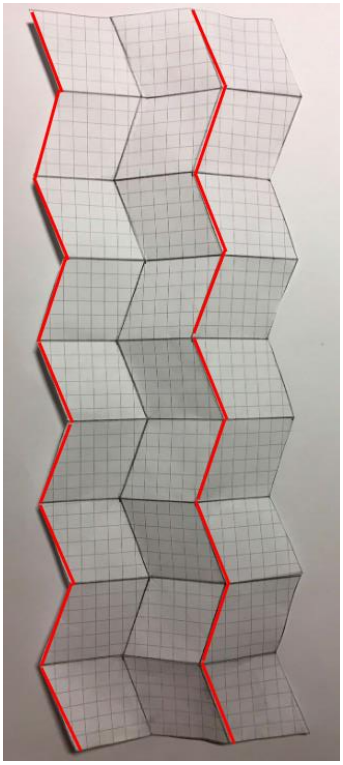

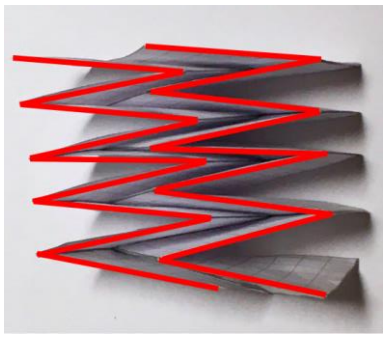

Figure 37: Figure 37 when folded

When *d* is smaller than *k*, the red lines in Figure 37 overlap as shown in Figure 38. These zig-zagging red lines represent the mountain folds running between the columns of parallelograms. When those mountain folds overlap in the fold, the thickness doubles in the areas of overlap, increasing the overall thickness.

Figure 38: Miura fold with d < k, unfolded

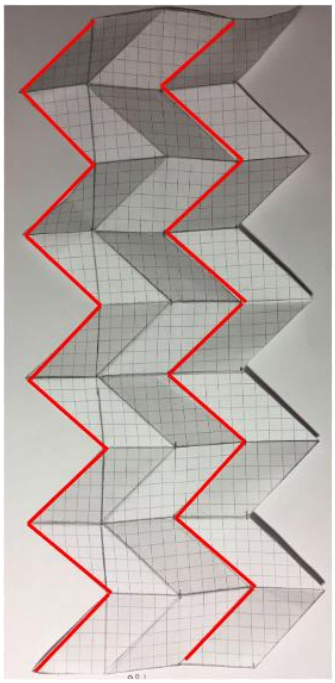

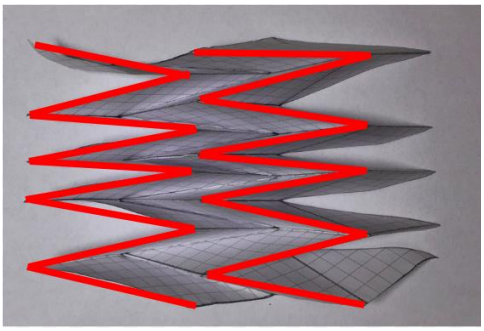

Figure 39: Figure 39 when folded

However, when *d* is equal to *k*, as in Figure 39, the mountain folds don't overlap, but are adjacent. This creates an even thickness across the whole fold (Figure 40). By choosing to keep *d* = *k*, this uniform thickness is ensured for all the possible folds with different values of *k*.

Figure 40: Miura fold with d = k, unfolded

The folded mat cannot be too long, either, as it should fit it in a regular hiking backpack. By fixing the length of the mat when folded to 60 cm, the value of *k* can be found which ensures both uniform thickness and a total length of about 60 cm.

For an odd-numbered Miura fold, the length when folded is given by:

$$(n_2 - 1) \times \left(\sqrt{k^2 + d^2}\right) - (n_2 - 2) \times \left(\sqrt{k^2 + d^2} - 2k \cos\left(\tan^{-1}\left(\frac{k}{d}\right)\right)\right)$$

$$= \sqrt{d^2 + k^2} - \frac{(-2n_2kd + 4kd)\sqrt{d^2 + k^2}}{d^2 + k^2}$$

Assuming *d* is equal to *k* this becomes:

$$\sqrt{2k^2} - \frac{2k^2(-n_2 + 2)\sqrt{2k^2}}{2k^2}$$

Simplified:

$$(n_2 - 1)k\sqrt{2}$$

n_2 times *k* is the width of the sleeping-mat when unfolded, which is 60 cm. Using this relationship, n_2 can be expressed by *k*:

$$n_2 = \frac{60}{k}$$

Substituting n_2 with this, and equating the length of the folded mat to 60, we get an equation with *k* as the only variable:

$$\left(\frac{60}{k} - 1\right)k\sqrt{2} = 60$$

$$60\sqrt{2} - k\sqrt{2} = 60$$

$$k = \frac{60\left(\sqrt{2} - 1\right)}{\sqrt{2}}$$

$$k = 17.6$$

The possible value of *k*, as a multiple of 180 and 60, closest to 17.6 is 20.

At $k = 20$, n_1 is 9, n_2 is 3, and $d = k = 20$.

The length of the folded mat will then be:

$$L(d) = \sqrt{d^2 + k^2} - \frac{(-2n_2kd + 4kd)\sqrt{d^2 + k^2}}{d^2 + k^2}$$

$$L(20) = 40\sqrt{2} = 56.6$$

$$\theta = \tan^{-1}\left(\frac{k}{d}\right) = \tan^{-1}\left(\frac{20}{20}\right) = 45°$$

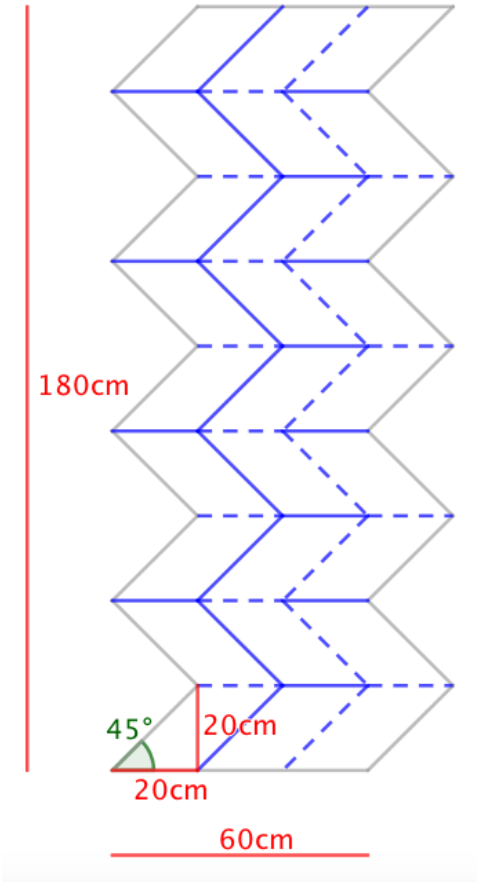

Figure 41: Finalized mat design

The optimal measurement of the width and the height of the parallelograms in the Miura fold of the sleeping-mat (Figure 41) are 20 cm, with the parallelograms being slanted at a 45-degree angle. When folded, this mat will have a parallelogram-shape with a length of 56.6 cm along the bottom.

Conclusion

In the first part of this investigation, Maekawa's theorem and Kawasaki's theorem were explained in relation to single-vertex flat-foldability in a Miura fold. These theorems hold true in all vertices of a Miura fold, yet are insufficient conditions to guarantee local flat-foldability. Bird's foot forcing provides insight into the limitations of flat-folding origami vertices, but has not yet been incorporated into a definite theorem.

Another interesting aspect of these folds that was not looked into is global flat-foldability, which is related to graph-theory and graph-colouring within discrete mathematics. There is also potential for further exploration into shape-memory of origami folds. It is unclear what the prerequisites are for a fold to have shape-memory, and this topic requires further research.

In the second part of this investigation, an attempt was made to incorporate the properties of a Miura fold into the design of a foldable sleeping-mat. This was done by creating an equation for the area of the folded sleeping-mat which included all the different variable measurements. The mathematics utilized throughout this process were a combination of geometry, trigonometry, algebra, and functions and equations.

A big challenge was ensuring that the fold would have no gaps, which was avoided by equalling the width and the height of the parallelograms. A minimum area of the folded mat could not be found while keeping it a Miura fold. Parameters were set in order to determine the best dimensions of the mat; consisting of limiting the slanting of the parallelograms to provide uniform thickness, and to set an approximate fixed width of the folded mat to ensure that it could fit inside a backpack.

Despite the final mat design having semi-uniform thickness, the relationship between the number of vertical parallelograms and the thickness of the fold is still unclear and could be investigated further. The volume of the sleeping-mat design created in this investigation is

unclear, and cannot be compared to existing sleeping mats to see if it is actually a more convenient design. Another limitation is that, due to the large inclination of the parallelograms, the unfolded mat has a very jagged shape which is impractical to sleep on. It is evident that there is much room for improvement in this design, and that more aspects will have to be considered in order to create a functional sleeping-mat.

Bibliography

Bain, I. (1980). The Miura-ori map. *New Scientist, London*. [online] Available at: https://www.britishorigami.info/academic/mathematics/the-miura-ori-map/ [Accessed 1 Dec. 2019].

Demaine, E. (2010). *Lecture 20 in 6.849: Geometric Folding Algorithms: Linkages, Origami, Polyhedra (Fall 2010)*. [online] Courses.csail.mit.edu. Available at: http://courses.csail.mit.edu/6.849/fall10/lectures/L20.html?images=16 [Accessed 5 Aug. 2019].

Garcia, X. (2017). *Tessellation and Miura Folds - Science Friday*. [online] Science Friday. Available at: https://www.sciencefriday.com/educational-resources/tessellation-and-miura-folds/ [Accessed 30 May 2019].

Hull, T. (1994). On the Mathematics of Flat Origamis. *Congressus Numerantium*. [online] Available at: http://www.organicorigami.com/thrackle/class/hon394/papers/HullOldFlatFoldabilityPaper.pdf [Accessed 1 Jun. 2019].

Hull, T. and Ginepro, J. (2014). Counting Miura-ori Foldings. *Journal of Integer Sequences*, [online] 17(10), p.3. Available at: https://pdfs.semanticscholar.org/3e5c/c622fb6062be07265736f29c8558a810c4a3.pdf?_ga=2.119286345.1387753678.1566636687-275455782.1566636687 [Accessed 24 Aug. 2019].

Landau, E. (2017). *Solar Power, Origami-Style*. [online] NASA. Available at: https://www.nasa.gov/jpl/news/origami-style-solar-power-20140814 [Accessed 1 Dec. 2019].

Natural Origami. (2016). *The Maekawa Theorem*. [online] Available at: https://naturalorigami.wordpress.com/2016/06/27/the-maekawa-theorem/ [Accessed 5 Jun. 2019].

Weisstein, E. (2019). *Isosceles Trapezoid -- from Wolfram MathWorld*. [online] Mathworld.wolfram.com. Available at: http://mathworld.wolfram.com/IsoscelesTrapezoid.html [Accessed 26 Aug. 2019].